Iranian Journal of Basic Medical Sciences

ijbms.mums.ac.ir

IJBMS

Design of eudragit RL nanoparticles by nanoemulsion method as carriers for ophthalmic drug delivery of ketotifen fumarate

Saieede Soltani [1, 2], Parvin Zakeri-Milani [3, 4], Mohammad Barzegar-Jalali [4], Mitra Jelvehgari [1, 4*]

[1] Drug Applied Research Center, Tabriz University of Medical Sciences, Tabriz, Iran
[2] Student Research Committee, Tabriz University of Medical Sciences, Tabriz, Iran
[3] Liver and Gastrointestinal Diseases Research Center, Tabriz University of Medical Sciences, Tabriz, Iran
[4] Department of Pharmaceutics, Faculty of Pharmacy, Tabriz University of Medical Sciences, Tabriz, Iran

ARTICLE INFO

Article type:
Original article

Article history:
Received: Dec 28, 2015
Accepted: Mar 3, 2016

Keywords:
Eudragit RL 100
Ketotifen fumarate
Nanoparticle
Ocular

ABSTRACT

Objective(s): Ketotifen fumarate (KF) is a selective and noncompetitive histamine antagonist (H1-receptor) that is used topically in the treatment of allergic conditions of rhinitis and conjunctivitis. The aim of this study was to formulate and improve an ophthalmic delivery system of KF. Ocular nanoparticles were prepared with the objective of reducing the frequency of administration and obtaining controlled release to improve the anti-inflammatory drug delivery.

Materials and Methods: In the present study, ocular KF loaded Eudragit RL 100 nanoparticles were prepared using O/W solvent diffusion method. The nanoparticles were evaluated for particle size, entrapment efficiency, surface morphology, X-ray diffraction (XRD), Fourier transform spectroscopy (FTIR), and differential scanning calorimetry (DSC). *In vitro* release and permeation studies were also carried out on nanoparticles.

Results: An average size range of 182 to 314.30 nm in diameter was obtained and encapsulation efficiency up to 95.0% was observed for all the formulations. Drug release for all formulations after 24 hr was between 65.51% and 88.82% indicating effective controlled release property of KF. The mechanism of drug release for best formulation was found to be fickian diffusion mechanism. KF nanoparticles containing high polymer concentration (1:15) presented a faster drug release and a higher drug penetration; on the contrary, nanoparticles containing low polymer concentration (1:7.5) were able to give a more sustained release of the drug and thus a slower KF permeation through the cornea.

Conclusion: The study revealed that KF NPs were capable of releasing the drug for a prolonged period of time and increasing the ocular bioavailability.

► *Please cite this article as:*
Soltani S, Zakeri-Milani P, Barzegar-Jalali M, Jelvehgari M. Design of eudragit RL nanoparticles by nanoemulsion method as carriers for ophthalmic drug delivery of ketotifen fumarate. Iran J Basic Med Sci 2016; 19:550-560.

Introduction

In conventional ophthalmic dosage forms, water soluble drugs are delivered in aqueous solution while water insoluble drugs are formulated as suspensions or ointments. Only 1-5% of the utilized drug penetrates into the cornea and achieves therapeutic concentrations in intraocular tissues. Low corneal bioavailability and low efficiency of drug penetration to the posterior segment of ocular tissue are some of the serious drawbacks of these systems. Drug is mostly drained away from the precorneal area in few minutes. Consequently, frequent instillation of concentrated solutions seems to be required for achieving desired therapeutic effects (1). Therefore recent research attempts have been focused on the development of novel and more effective delivery systems. Nanosuspensions have been brought to light as a promising dosage form for ocular use (2). Decreasing the particle size of drugs has been an effective and valid manner for modifying the bioavailability of insoluble drugs. Nanosuspension has appeared as an efficient and favorable tactic for delivery of insoluble drugs due to its distinctive advantages such as simple improving, procedure flexibility, targeting abilities, and changed pharmacokinetic profile. These special aspects of nanosuspension have allowed its utilization in different dosage forms, containing dedicated delivery systems such as oral, parenteral, ocular and pulmonary routes (3-5).

Nanosuspensions are submicron colloidal dispersions of separate particles that have been fixed by using polymers, surfactants, or admixture of both (6).

*Corresponding author: Mitra Jelvehgari. Department of Pharmaceutics, Faculty of Pharmacy, Tabriz University of Medical Sciences, Tabriz, Iran. Tel: +98-41-3339-2585; email: mitra_jelvehgari@yahoo.com; jelvehgri@tbzmed.ac.ir; mjelvehgari@gmail.com

The particle size range of nanosuspension is between 200 and 600 nm (5). Dispersion phase can be water, aqueous solutions or non-aqueous medium. Currently, nanoparticle technology is being utilized on trade scale in drug delivery to dominate solubility problems.

The aqueous surfactant solution Polyvinyl alcohol (PVA) contains a dispersion of surfactant micelles distributed throughout the water phase. Presence of surfactants helps in lowering the surface tensions between two phases (7).

Pignatello *et al* improved the stability of cloricromene loaded polymeric nanosuspensions of Eudragit RS 100 and RL 100 by quasi-emulsion solvent diffusion method (8). They showed that cloricromene loaded nanosuspensions suggest an indicating strategy to develop the stability and bioavailability of the drug (8).

Eudragit RL nanosuspensions have been reported to demonstrate a reliable carrier system for the ophthalmic release of drugs such as ibuprofen and flurbiprofen (9, 10). Such drug loaded carrier systems display desirable stability characteristics and size distribution, and a positive surface charge, which has made them potential ocular drug delivery systems. Especially, the positive surface charge of these nanoparticles can allow a sustained residence time on the corneal surface, satisfying gradual drug release and better aqueous humor drug (11).

The white to brownish-yellow, fine crystalline powder, ketotifen fumarate (KF) is sparingly soluble in water. KF is a relatively selective, noncompetitive histamine antagonist (H1-receptor) and mast cell stabilizer that is locally used in the treatment of allergic conditions such as rhinitis and conjunctivitis (12).

Conventional ophthalmic solutions often eliminate rapidly after administration and cannot provide and maintain an adequate concentration of the drug in the precorneal area (13). Ocular bioavailability of topical drugs is very poor and there are inherent problems such as patient non-compliance (14). Only 1%-5% of the topically applied drugs reach the intraocular tissue, while the remainder of the instilled dose undergoes a nonproductive absorption by the conjunctiva or drainage via the nasolacrimal duct. This results in drug loss into the systemic circulation and provides undesirable systemic side effects (15).

Eudragit RL or Eudragit Retard L polymer is a copolymer of poly (ethylacrylate, methyl-methacrylate, and chloro trimethyl-ammonioethyl methacrylate) which contains an amount of quaternary ammonium groups between 8.8% and 12%. It is insoluble at physiologic pH values and has limited swelling. Therefore, Eudragit RL is represented as a good material for the dispersion of drugs. Its positive charge can allow a longer residence time of nanoparticles (NPs) on the corneal surface.

The challenging objective was to develop the nanosuspension of KF for topical drug delivery systems with improved ocular retention, increased corneal drug permeation, and reduced irritation.

Materials and Methods

Eudragit RL 100 was a kindly gift from Akbarie Co. (Evonik Ind. (Darmstadt, Germany). KF was purchased from Behansar Co, Iran. Polyvinyl alcohol (MW 72000), D-mannitol, ethanol, and sodium chloride, calcium chloride, potassium chloride were obtained from Merck (Germany) and commercial eye drop Zaditen® (0.025%) was supplied by Thea pharma (France). All solvents and reagents were of analytical grade.

Nanoparticles preparation

KF loaded nanocarriers were prepared by means of solvent diffusion (O/W) method at different drug to polymer ratios (1:7.5, 1:10, 1:15). At first, drug and polymer were dissolved in 12 ml ethanol and organic solution was emulsified in 25 ml of 1%w/v PVA aqueous solution using 80% power of ultrasound probe (Hielscher, UP200H) for 3 min. Then the O/W emulsion was diluted in 50 ml distilled water for better ethanol diffusion. Finally resulted emulsion was stirred for 24 hr at room temperature to extract organic solvent. Prepared nanosuspension was mixed with 10 ml 5%w/v mannitol solution as a cryoprotectant and lyophilized. Before adding mannitol, 7 ml of nanosuspension was taken for loading analysis (Figure 1). The blank nanoparticles (NPs) (without the drug) were prepared under the same conditions as above without using drug.

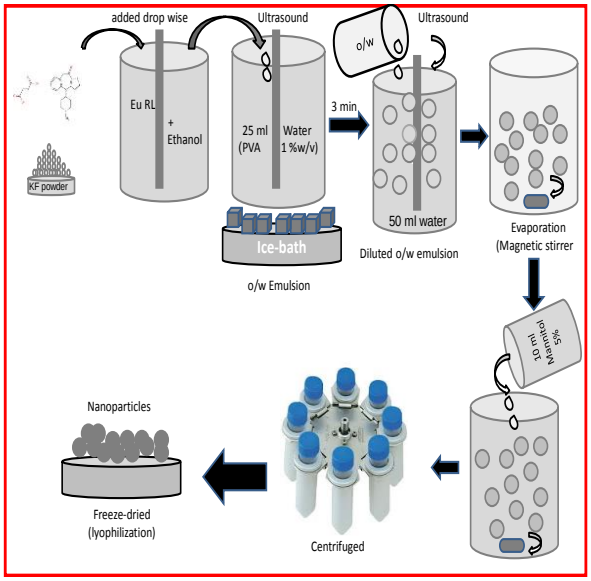

Figure 1. Nanoparticles preparation procedure with Eudragit RL 100 polymer

Characterization of NPs

Particle size and zeta potential

Particle size and zeta potential of freshly prepared nanosuspension were determined by Dynamic Light Scattering (Malvern, UK) using a Zetasizer Nano ZS (Malvern, UK).

Morphology

Scanning electron microscopy (SEM, MIRA3 TESCAN, Czech Republic) was used to examine the surface morphology of Eudragit nanoparticles. The NPs were mounted on a metal stub with a double adhesive tape and coated with platinum/palladium alloy under vacuum (30 kV).

Drug loading and production yield of NPs

To determine the drug loading efficiency and production yield of nanoparticles, 7 ml of prepared nanosuspension were separated using Amicon 30000MWCO centrifugal filters (4000 rpm, 45 min). The supernatant was UV analyzed for unloaded drug at 298 nm wavelength. Calibration curve was performed by means of KF in 1% PVA aqueous solution. The drug loading and production yield were determined using the following equations:

Drug loading efficiency= (Total amount of drug-unincorporated drug amount)/ Total amount of drug ×100 (16).

The production yield of the NPs was determined by dividing the final weight of the polymeric particles to the initial weight of the raw materials. Each determination was performed in triplicate.

Evaluation of physical state and polymer-drug interaction of NPs

Physical state and polymer-drug interaction of NPs were examined by XRD, DSC and FTIR analyses.

X-ray diffraction (XRD)

XRD analysis result was obtained using Bruker Axs, D8 Advance diffractometer with nickel-filtered CuKα radiation (operating at 40 KV, 20 mA). The scanning rate was 4°/min over a 2θ range of 10°-90°.

Differential scanning calorimetry

Differential scanning calorimetry (DSC) (Shimadzu, Japan) measurements were carried out on drug, polymer, and PVA, as well as on different formulations. The weighed samples were put in aluminum pans and were scanned from 30 °C to 300 °C with heating rate of 10 ˚C/min.

Fourier transforms infrared spectroscopy

The FT-IR spectra for KF loaded nanoparticles, blank NPs, polymer and drug were obtained by a computerized Fourier transform infrared spectroscopy Tensor 27 (Bruker, Germany) operating in the scanning wavenumber range of 400-4000 cm^{-1} at 1 cm^{-1} resolution.

***In vitro* release study**

In vitro release

In vitro release experiments were performed on Eudragit NPs using dialysis bag diffusion method (17). An amount of 50 mg of particles were suspended in 4 ml water in dialysis bag (cut off 12,000 Da), which was immersed in 300 ml simulated lacrimal fluid (SLF) buffer (pH 6.8) (8.3 g NaCl, 0.084 $CaCl_2$, $2H_2O$ and 1.4 g KCl for one liter) as dissolution medium. The medium was preheated to 32±1˚C and stirred at 100 rpm. At preset intervals, 3.5 ml of medium were withdrawn and replaced with 3.5 ml of fresh SLF to keep the sink condition for 24 hr. The amount of KF in the samples was determined by UV/Vis spectrophotometer (Shimadzu-160, Japan) at 298 nm wavelengths. The experiments were repeated three times for each formulation.

To have a better comparison between different formulations, dissolution efficiency (DE), $t_{50\%}$ (dissolution time for 50% fraction of drug), dissolution efficiency (the area under the dissolution curve up to a certain time, t, expressed as a percentage of the area of the rectangle arising from 100% dissolution in the same time) and different factor, f1 (used to compare multipoint dissolution profiles) were calculated using the following equation:

$$f1 = ([\sum_{t=1}^{n} Rt - Tt) / [\sum_{t=1}^{n} Rt)] \times 100$$

Where n is the number of time points at which percentage dissolved was determined, R_t is the percentage dissolved of one formulation at a given time point and T_t is the percentage dissolved of the formulation compared at the same time point. The difference factor should be between 0 and 15 when the test and reference profiles are identical, and approaches above 15 as the dissimilarity increase.

In vitro release kinetics

In order to study the kinetics and mechanism of drug release from NPs, the resultant data from release experiments were fitted to different kinetic models such as zero order, first order, Higuchi, Hixson Crowell, and Korsmeyer-Peppas, and analyzed. Data obtained from *in-vitro* release studies were fitted to various kinetic equations to find out the mechanism of drug release from the Eudragit Rl100 nanoparticles. The kinetic models used were:

$Q_t = k_0 t$ (zero-order equation)

$\ln Q_t = \ln Q_0 - k_1.t$ (first-order equation)

$Q_t = K.S.t^{0.5} = k_H.t^{0.5}$

(Higuchi equation based on Fickian diffusion)

Here, Q is the amount of drug release in time t, Q_0 is the initial amount of drug in the nanoparticles, S is the surface area of the nanoparticle and k_0, k_1 and k_H are

rate constants of zero order, first order and Higuchi equation, respectively. In addition to these basic release models, the release data was fitted to the Peppas and Korsmeyer equation (power law):

$Mt/M\infty = k.t^n$

Here, M_t is the amount of drug release at time t and $M\infty$ is the release at time $t = \infty$, thus $Mt/M\infty$ is the fraction of drug released at time t, k is the kinetic constant, and *n* is the diffusion exponent which can be used to characterize the mechanism of drug release.

Ex-vivo transcorneal permeation studies

The *in vitro* permeation of the KF NPs through the bovine corneas was studied using Franz diffusion cell at 32 °C. The scleral layer of the freshly obtained cornea was mounted between the donor and the receptor compartments. The 50 mg NPs suspended in 5 ml distilled water were placed on the epithelial faced surface and the compartments were clamped together. The nanosuspension was placed on the cornea in the donor compartment and was sealed with a glass cover slip and soaked with simulated lacrimal fluid (SLF, composition: 8.3 g of NaCl, 0.084 g of $CaCl_2 \cdot 2H_2O$, 1.4 g of KCl, and distilled deionized water to 1000 ml). The receptor compartment was filled with 22-25 ml SLF at pH 6.8, and stirred with a magnetic bead at 200 rpm (18, 19). Three milliliters of sample were withdrawn at predetermined time intervals and replaced with 3 ml of fresh medium. The drug concentration was analyzed for drugs at 298 nm.

Permeability coefficient was calculated using the following equation:

$$Kp = \frac{Jss}{C_0}$$

Where Jss is the steady state flux per unit area, Kp is the permeability coefficient for a given solute in a given vehicle (cm h^{-1}), and C_0 is the concentration of the solute in the donor compartment.

Statistical analysis

Where appropriate, all results were evaluated using a one-way ANOVA or t-test at the 0.05 level of probability.

Results

The effect of drug to polymer ratio n particle size, zeta potential, and entrapment efficiency of nanoparticles is shown in Table 1. The particle size ranged from 182 nm (Formulation F_1) to 117 nm (Formulation F_3) which was prepared using the higher amount of polymer in the organic phase. The increase in amount of polymer in the organic phase resulted in significant differences in particle size (Table 1).

The polydispersity index (PDI) is considered as an indicator for particle size distribution. For submicron particles PDI value in the range of 0.15-0.3, indicates size homogeneity, while a PDI value higher than 0.3 implies heterogeneity.

The mean PDI values for the drug loaded formulations varied in the range of 0.3-0.66. All batches represented the small mean size, suitable for ocular application. The nanosuspensions exhibited positive zeta potential values (Table 1) ranging from +6.58 to +13.40 mV.

SEM images of Eudragit RL 100 nanoparticles are shown in Figure 2. The prepared Eudragit RL 100 nanoparticles were nearly spherical in shape with a smooth surface (Figure 2). In the present experiment, the drug loading capacity values of KF in the Eudragit RL 100 nanoparticles with different drug to polymer ratios (1:7.5, 1:10, 1:15) were 11.03%, 8.56% and 5.94% and the corresponding entrapment efficiencies were 93.95%, 94.32% and 95.23%, respectively (Table 1).

Physicochemical characterization

FTIR analysis

Pure KF has characteristic IR peaks of vibration N-H at 3424.64 cm^{-1}, aromatic stretching vibration C=C at 1649.70 cm^{-1}, bending vibration CH_3 at 1476.99 cm^{-1}, bending vibration phenolic OH at 1397.14 and CH out of plane bending vibrations in substituted ethylenic system (-C=CH- (cis) at 754.15 cm^{-1} (Figure 3). The spectra produced by FTIR for the Eudragit RL100 are presented in Figure 3. One can observe, in the spectra, the strong bands in the region between 1150-1190 cm^{-1} and 1240-1270 cm^{-1}, due to the stretch of carbonyl (ester) groups present in the Eudragit. There are also stretching bands of C(=O) ester vibration at 1734.01 cm^{-1}. The 1388.22, 1449.97, 2953 and 2992.11 cm^{-1} bands in the FTIR spectra can be discerned to CHx vibration. IR absorption frequency of OH stretch at 3437.91 cm-1 is presented in Figure 3.

In the FTIR spectra of the blank NPs of F_2, peaks were observed at wavenumbers 3304, 2935, 1728.93, 1436.58, 1089.83, and 845.02 cm^{-1}. FTIR studies showed the characteristic peaks of KF, confirming the purity of drug.

For NPs, stretching strong band C-H (alkyne group) are seen at 3293.88-3298 cm^{-1}, stretch band C-H (alkane group) at 2936.61, 2937.50 and 2939.24 cm^{-1}, N-H stretch band of the amine group at 3295 cm^{-1}, stretch band of carbonyl group at 1728.54, 1728.79 and 1729.01 cm^{-1}, bending vibrations in -C-H at 1436.12, 1436.62 and 1438.91 cm^{-1}, stretch band of ester group C-O at 1089.41, 1089.61 and 1090.74 cm^{-1}, and stretch band in -C-Cl at 844.76, 845.12, and 845.57 cm^{-1}.

Table1. Effect of various drug to polymer ratio on particle size, zeta potential, and entrapment efficiency of KF loaded Eudragit RL 100 polymeric nanoparticles

Formulation number	Drug to polymer ratio	Theoretical drug content (%)	Encapsulation efficiency (%±SD)	Mean particle Size (nm)	Polydispersity Index (±SD)	Zeta potential (mV±SD)
F_1	1:7.5	11.76	93.95±5.23	182.00±26.02	0.733±0.09	+6.580±0.40
F_2	1:10	9.10	94.32±7.65	134.53±37.47	0.336±0.11	+11.05±3.11
F_3	1:15	6.25	95.23±8.45	117.00±16.00	0.434±0.18	+13.40±0.28
Blank NPs of F_2	-	-	-	106.70±00.00	0.473±0.00	+22.60±0.00

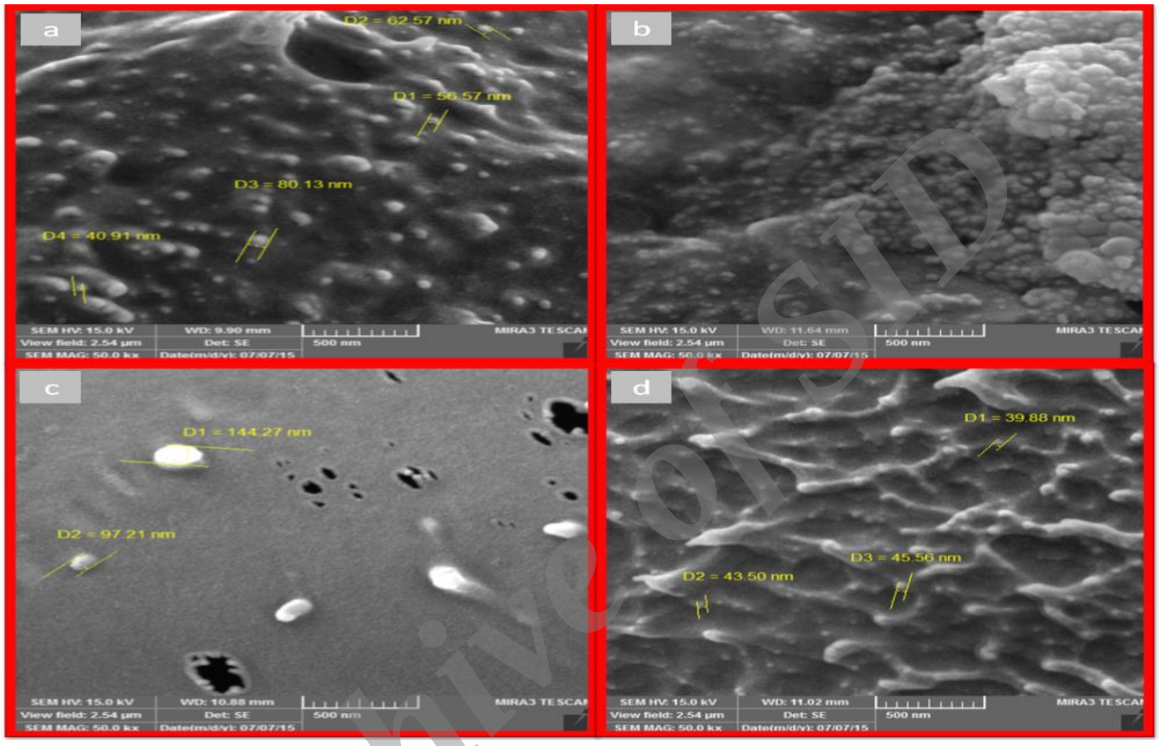

Figure 2. SEM images of nanoparticles containing KF (a) F_1 (KF: Eudragit) 1: 7. 5, b) F_2 (KF: Eudragit) 1:10, c) F_3 (KF: Eudragit) 1:15, d) blank F_2 at 15000× magnification

DSC analysis

From the DSC thermograms, it was observed that KF is crystalline in nature (Figure 4). It exhibited a sharp melting endotherm at an onset temperature of 197.69 ˚C, a peak temperature of 201.09 ˚C, and a heat of fusion of 176.14 J/g. Eudragit RL 100 polymer which is found as an utterly amorphous form with a glass transition temperature (Tg) of about 60˚C.

The freeze dried drug loaded NPs showed a broad endothermic transition at an onset of 216.68 ˚C, a peak at 197.93˚C and a peak at 213.96˚C (from F_1 to F_3).

PXRD analysis

In order to investigate the physical nature of the encapsulated drug, the powder X-ray diffraction technique was used. Solid state analysis of the NPs after freeze drying showed that the drug has dispersed in the polymeric matrices in a semicrystalline to microcrystalline form. Since the polymer is completely amorphous in nature, entrapment of the crystalline KF (sharp intense peaks as seen in Figure 5) into the polymeric nanoparticles reduced its crystallinity to a greater extent. Similar observation has seen for all NPs. This is evident from the disappearance of most peaks in the nanoparticles compared to the drug.

In vitro release studies

In vitro drug release (as shown in Figure 6) compares the release of KF from the Eudragit RL 100-based nanosuspension. The release of KF was evaluated by dialysis, using simulated lachrymal fluid (pH 6.8) as the release medium.

The NP formulations made with the drug to polymer ratio of 1:7.5, 1:10 and 1:15 showed 30.68%, 55.63%, and 62.29% drug release in 15 min and 64.80%, 79.64%, and 87.65% release in 8 hr while 101.72% drug was diffused into the release medium in 15 min from a Zaditen® drop used as a control (0.345 mg/ml).

The release curve of NPs suggests an initial fast release. This may be due to the unentrapped drug being adsorbed on the surface of the NPs. The result suggests that entrapment of the drug in the NPs hinders the drug release which is biphasic; an initial burst release is followed by a slow release phase, as the drug to polymer ratio is changed from 1:7.5 to 1:15 (as the polymer concentration is increased).

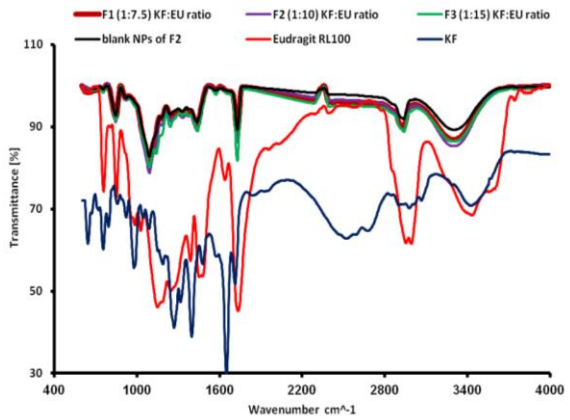

Figure 3. FTIR thermogram from down to up Ketotifen fumarate; Eudragit RL 100; PVA; blank NPs of F_2; F_1 (KF:EU) 1:7.5 ratio; F_2 (KF:EU) 1:10 ratio; F_3 (KF:EU) 1:15 ratio, respectively

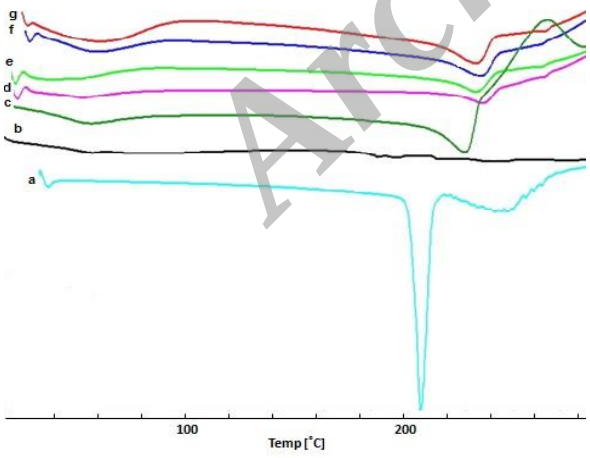

Figure 4. DSC thermogram of Ketotifen fumarate (a); Eudragit RL 100 (b); PVA (c); blank NPs of F_2 (d); F_1 (KF:EU) 1:7.5 ratio (e); F_2 (KF:EU) 1:10 ratio (f); F_3 (KF:EU) 1:10 ratio (g), respectively

Statistical analyses of data were performed by comparing the DE (dissolution efficiency), $t_{50\%}$ (dissolution time for 50% fractions of drug), the difference factor, and f_1 (Table 2).

Dissolution efficiency (DE) was calculated from the area under the dissolution curve at time (measured using the trapezoidal rule) and was expressed as percentage of the area of the rectangle described by 100% dissolution in the same time. F_1 NPs showed a lower slow dissolution efficiency of 61.28%. KF drop had a higher release in comparison with NPs (Table 2 & Figure 6) (P<0.05), and an increase in DE (101.03%) was significant compared to NPs (P<0.05).

The difference factor displayed that the NPs formulations did not match the release profile of commercial formulation (Table 2) and there was a significant difference between these two dissolution profiles ($f1$ = 20.22-49.24).

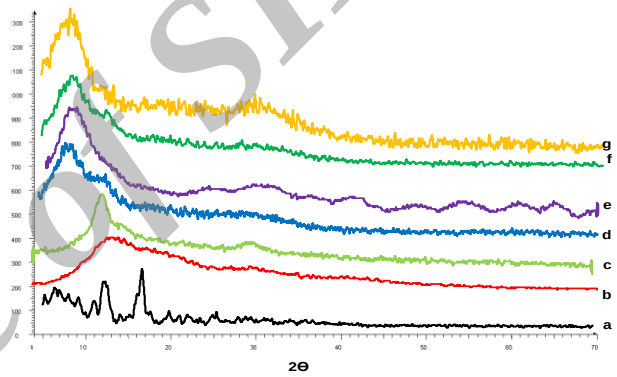

Figure 5. XRD thermogram of Ketotifen fumarate (a); Eudragit RL 100 (b); PVA (c); blank NPs of F_2 (d); F_1 (e); F_2 (f); F_3 (g), respectively

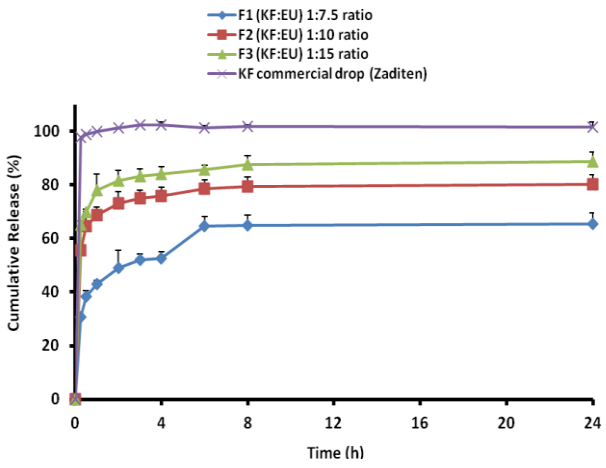

Figure 6. Cumulative percentage of KF release from naoparticles with different polymer ratios and KF commercial drop

Table2. Comparison of various release characteristics, flux and permeability coefficient of KF from different NPs formulations and commercial® drop

Formulation	[a]$Rel_{0.25}$ (%±SD)	[b]Rel_8 (%±SD)	[c]DE	[d]$T_{50\%}$ (min)	[e]f_1	[f]Flux [(mg/cm².min)*10⁻³±SD]	[g]Kp [(cm/min) *10⁻⁴±SD]
F_1	30.67±1.54	65.51±4.10	61.28	93	49.24	0.6±0.012	10.7±0.89
F_2	55.74±5.28	80.31±3.48	77.77	45.64	28.19	0.6±0.009	16.78±1.23
F_3	65.14±1.44	88.82±3.33	85.88	46.61	20.22	0.5±0.005	17.30±1.78
KF drop®	97.77±0.00	101.62±1.81	101.03	8.31	0	0.1±0.002	28.99±2.33

[a] $Rel_{0.25}$ = amount of drug release after 0.25 hr; [b] Rel_8 = amount of drug release after 8 h; [c]DE = dissolution efficiency; [d]t 50% = dissolution time for 50% fractions; [e] f_1 = Differential factor ($0<f_1<15$), KF drop®= Reference product, [f]Flux: amount of drug released per unit surface area versus time, [g]permeability coefficient

Table3. The best fitting parameters of *in vitro* release data to kinetic models

Formulation	ORDER	MPE%	RSQ	k	n	Slope	Intercept
F1	Peppas	2.96	0.970	0.1915	0.192	0.192	-1.653
F2	Weibull	2.58	0.913	0.0366	-	0.152	-0.502
F3	Weibull	1.99	0.941	0.1338	-	0.169	-0.340
KF drop®	Weibull	0.00	1.000	14.2670	-	0.249	0.662

The drug was gradually released at a later stage, and the rate of which was declared by the diffusion of the drug in the flexible matrix structure. The values of dissolution models offer that the drug release may occur mainly through diffusion processes. Peppas and Weibull kinetic models (Table 3) show the highest correlation; as it is evident from the values of regression coefficients (R^2) for F_1, F_2, and F_3 NPs as 0.970, 0.913 and 0.941, respectively.

Ex vivo transcorneal permeability

Permeation data of KF from ophthalmic NPs are represented in Table 2. The data reveals that the drug permeability increases with the concentration of Eudragit from 75 to 150 mg. It is worth mentioning that an increase in the permeation was observed with increasing the concentration of Eudragit RL, though.

Discussion

When Eudragit nanoparticles are to be formed by the emulsification-diffusion technique, the organic solvent phase containing Eudragit polymer as well as the aqueous phase containing stabilizer (PVA) are in the state of thermodynamic equilibrium. The addition of water to the system upsets the equilibrium. It causes the diffusion of organic solvent to the external phase. During the transport of the solvent, Eudragit NPs are produced with their size possibly dependent on the type of organic phase solvent. Polyvinyl alcohol (PVA) as a hydrophilic biocompatible polymer is used as surfactant for production of NPs (20). PVA forms a hydrophilic layer at the NPs surface providing stability of the colloidal system and improving NPs resistance to freezing as well as their redispersion after freeze-drying (21).

The instability of the nanosuspensions after a long storage period is one of the main problems that limit the use of these systems. To overcome the problem, the water content of formulations must be removed by either Lyophilization or freeze-drying. The liquid nanosuspension is frozen and then, under vacuum, the water is removed by sublimation and desorption. Lyophilization could generate enormous stresses that could destabilize NPs, and alter their physicochemical characteristics. Thus, to avoid such possible alterations, cryoprotectants or lyoprotectants (as manitol) are usually added to the formulation (22).

A small mean size was observed in all NPs, well suited for possible ocular application to prevent patient discomfort and provide a good drug diffusional release. Particle size for ophthalmic applications should not exceed 10 µm because with larger sizes a scratching feeling might occur (23). Therefore, a reduced particle size improves the patient comfort.

The smaller particle size with an increase in the polymer concentration was probably due to increase the surfactant (PVA) concentration, resulting in smaller nanodroplets formation in NPs ensures good emulsification process and results in both size reduction and a lower polydispersity index (24).

The zeta-potential measurement is used as a remarkable surface-characterization technique which supplies information around the surface charge of nanoparticulate systems. In a specific liquid medium, zeta potential measures the charge on a particle surface. Measuring the surface charge by zetapotential technique assists in comprehending and predicting interactions between particles of suspension. The magnitude of zeta potential is indeed indicator of the potential stability of colloidal system. A zeta potential

value of ±30 mV may sufficiently contribute to the physical stability of suspension (25, 26).

The surface of NPs reaches a positive charge in result of presence of the quaternary ammonium groups on Eudragit RL 100. This is consistent with the findings of Pignatello *et al* (27). Mandal *et al* also reported that sulfacetamide loaded Eudragit RL100 nanosuspensions had spherical and uniform particles with positive zeta potential (+24.1 mV). The results indicate that the formulation of nanosuspension could be utilized as potential delivery system for treating ocular bacterial infections (28). Pignatello *et al.* Showed that cloricromene-loaded Eudragit RL nanoparticles obtained with size mean (80 nm), polydispersity (0.719) and surface charge values (+ 27.3 mV), were suitable for ophthalmic application (29).

As mucin layer on corneal surface is negatively charged, the positively charged NPs could help in effective adhesion to the corneal surface which in turn would enhance the ocular bioavailability.

These particles are unlikely to cause any irritation to the ocular surface, as it is understood that isometric particles with obtuse angles and edges correlate with less irritation than the particles with sharp angles and edges (30).

Increase in the polymer concentration (from 75-150 mg) increased drug entrapment efficiency. As the polymer concentration in organic phase increases, negligible increase in drug entrapment efficiency occurs due to the increase in the organic phase viscosity (Table 1), which inhibits the movement of drug molecules from organic phase to aqueous phase. The increase in entrapment efficiency with the drug to polymer ratio of 1:15 seems to be due to an increase in drug loading capacity, as entrapment efficiency is the ratio of actual drug loading and initial amount of drug. Based on the results, the formulation made with 1:10 drug to polymer ratio (F_2) was selected for further studies. The increased entrapment efficiency, small size, good polydispersity, high release and flux could be linked to the formation of stable emulsion and formation of uniform dispersion which enhanced the drug encapsulation efficiency and stopped drug loss.

Differences in absorption bands positions of KF were observed in spectra of the prepared formulations, indicating that there are intermolecular hydrogen bonding interactions between ketotifen fumarate and Eudragit RL 100 (31). It could be the proof of chemical stability of the drug inside the NPs. Furthermore a new band in 1572 cm^{-1} in the spectra of NPs may result from intermacromolecular ionized bonds between fumaric acid and Eudragit RL sequences (Figure 3).

The thermal behavior of the freeze dried NPs proposed that the polymer prevented the melting of drug crystals. The ionic interaction may have occurred in the NPs as observed for the KF and Eudragit RL 100 system (32). Shifting the Tg of Eudragit RL is due to its interaction phenomena with fumaric acid. It is possible that the dominant interaction in the solid state could be protonation of the deprotonated fumarate in KF by the acidic proton of Eudragit RL100. In the freeze dried nanoparticles, the peak of KF was disappeared indicating possibility of conversion of drug into amorphous form. The drug molecules might have entirely been dispersed in the polymer matrix. According to the literature, decrease in crystallinity of the drug exhibits more solubility (33, 34).

In the thermogram of the Eudragit RL-based NPs, there was a small endothermic peak at 220–222 °C which corresponds to the phase transition of PVA (Figure 4). Based on thermodynamic calculations on the enthalpy of this endotherm, the heat flow of PVA in NPs was obtained (26.93, 38.32 and 41.83 J/g for F1, F2 and F3 formulations, respectively) (Figure 4). This can be explained based on the effect of adsorbed PVA as surfactant onto the drug loaded NPs. PVA exhibited Tg value of 50˚C, a melting onset of 209.35˚C and a peak of 219.74˚C with degradation at more than 225˚C consistent with the finding of Zakeri *et al* (35).

The most probable reason for the appearance of slightly shifted broad endothermic peak and exothermic peak is the melting or crystallization of adsorbed PVA present on the NPs surface.

There may also be the possibility of overlapping of drug peaks by the background diffraction pattern of the amorphous structure (36). Thus, it can be concluded that the drug is present inside the NPs in the semicrystalline to microcrystalline form. This finding was also in agreement with the flurbiprofen loaded acrylate polymer nanosuspension prepared by Pignatello *et al* (27). Reducing the intensity of drug peaks in freeze-dried NPs was possibly happened due to the interaction phenomena between Eudragit RL and KF base (by increasing Eudragit RL weight fraction from F1 to F3 formulation, the intensities of typical drug peaks were lowered due to the dilution effect exerted by the polymer network). This supports the results obtained from FTIR and DSC.

Pignatello *et al* indicated that the drug release from Eudragit® RL 100 particles was intricate in nature as it involved the occurrence of dissolutive and diffusive phenomena (4, 27). Overall the drug release rate of F3 (with 93.75% polymer) was more than that of F2 and F1 (with 90% and 88.24% polymer, respectively) which is probably due to the high water permeability and swellability of Eudragit®. The presence of a high content of quaternary ammonium groups makes the polymer permeable to water, increases the porosity of the matrix (in F3 formulation (with high polymer concentration) than in F1 and F2 formulations), and accelerates the drug release.

Such findings can be related to progressive saturation of the polymer ammonium group by drug molecule occurring at higher drug to polymer ratio, which increases the dissolutive nature of drug release. According to the results, increasing the molar amount

of polymer leads to increasing the amount of complex Eudragit RL100-fumaric acid and possibly provides hydrophilicity of prepared systems. This result is in accordance with the prior studies of Pignatello et al (3, 27).

The release profiles were fitted to Peppas (n<0.5) and Weibull, indicating diffusion mechanism which was expected to control the drug release. In Weibull model, it is considered that some of the factors affecting the overall drug release e.g. effective surface area (S) are rarely mass dependent, mass of unreleased drug in the medium, while the others are supposed to be time dependent. This result was also supported by previous studies on RL NPs displaying that drug release is always the result of both dissolutive and diffusional phenomena. Rate of drug release increased for high concentration of polymer (1:15 ratio) in F3 formulations for the first 0.25 hour. This also may be due to the presence of un-loaded drug on the surface of the NP.

The higher burst release could be due to the fact that increased PVA (according to DSC data, loading order of PVA in NPs formulations; F3>F2>F1) resulted in decreased average particle size (F3), which increased the effective surface area exposed to the drug release media, subsequently resulting in increased initial release. The dissolution and release of surface-bound PVA molecules caused the initial high release of F3 formulation. High PVA proportion also increased the loading efficiency in the NPs formulation, which further contributed to the increased burst release (65.14%). The formulations (F1 & F2) with lower proportion of PVA showed higher average particle size (182 and 134.53 nm, respectively) and lower loading efficiency; hence a decreased burst release (30.67% and 55.74%, respectively) and a prolonged release of drug was observed.

The NPs (drug to polymer ratio of 1:7.5) were freeze-dried since they had the highest drug loading capacity (4.47%) with a small particle size (182 nm) and sustained release behavior in 8-12 hr (65.51%). Particle size is a critical factor for NPsbased drug delivery system. The particle size of formulations (from F1 to F3) was 182 to 117 nm. As the particle size decreases, the surface area of the particles increases; thus increases the dissolution rate of drug. Therefore, the smaller the particle size, the higher the dissolution rate (F3).

Using mannitol as cryoprotectant resulted in a white spongy, cotton-like material upon lyophilization. The sample freeze-dried without cryoprotectants did not redisperse in water after manual hand shaking; therefore, large aggregates were observed. Further, mannitol containing samples showed redispersibility upon the manual shaking (37).

The drug was gradually released at a later stage, and the rate of which was declared by the diffusion (n<0.5) of the drug in the flexible matrix structure. The values of dissolution models offer that the drug release may occur mainly through diffusion processes (38).

Eudragit RL 100 is the copolymer of acrylic and methacrylic acid esters with hydrophilic ammonium groups which improve the permeability as a channeling agent for the entrance of the liquid medium through the dispersed NPs wall, causing it to swell. This simplifies the diffusion of the loaded drug out of the NPs into the dissolution medium.

The present study demonstrated the influence of different concentrations of Eudragit RL polymers on NPs permeation rate. The substances diffusion through the epithelial barriers depends not only on the properties involved but also on the chemical nature, size and conformation, lipid-water partition coefficient, degree of ionization of the penetrative molecules tested and so on (4, 27). For molecular diffusion studies, the cornea may be considered as consisting three primary layers (i.e epithelium, stroma, and endothelium). Whatever is the physicochemical property of the penetration, the diffusional resistance offered by the individual layers may widely differ. Epithelium which is lipid in nature and consists of roughly five layers of epithelial cells is the main barrier, rendering high resistance to the diffusion of ionic or relatively hydrophobic agents. The aqueous stroma, which encompasses the bulk of the cornea in mass and thickness as well, is the major rate-limiting barrier to the diffusion of hydrophobic agents. The KF-loaded Eudragit NPs showed a higher drug permeation coefficient 0.6 (mg/cm^2.min ±0.012) compared with the commercial marketed eye drops 0.1 (mg/cm^{2}min±0.002). KF from commercial formulation was permeated 57.54% in 8 hr whereas KF from RL nanoparticles was permeated 40.10-67.22% in 8 hr. KF loaded Eudragit NPs shows a significantly ($P<$ 0.05) higher permeation capability as compared to the commercial eye drops. This admired penetration of KF across the cornea could be the result of agglomeration of the NPs in the conjuntival sac; thus forming a depot from which the drug is gradually delivered to the precorneal area. The results suggest possible corneal uptake of the NPs due to the positive charge and small size. The cationic characteristics of Eudragit® RL and positive charges of NPs cause ionic interaction with the negatively charged mucus layer at the eye surface. Positively charged surfaces offer the prospects of lengthening the residence time of NPs in the cul-de-sac and consequently ensuring optimal contact between the formulation and the eye (39). In the case of ocular application, it is hard to sustain the therapeutic effects for a significant time span because the liquid dosage forms very readily are removed from the eye. As a result of corneal uptake of the NPs, cornea acts like a reservoir and KF releases in a controlled behavior. Besides, the burst release would certify an ample drug level just after instillation. It could be expected that KF would precipitate within the limited volume of lacrymal

fluid present in the precorneal environment due to the burst release and accumulate in the dead end (39). In that case, the precipitated KF would also act like a reservoir and redissolve slowly in the lacrymal fluid, hence leading to a constant release of KF. The long-term release of the KF would lead to an increase in efficiency of the treatment.

Conclusion

Eudragit RL 100-based KF nanoparticles prepared by nanoemulsion method with different drug to polymer ratios showed high entrapment efficiency, low poly dispersity index and positive zeta potential. Thus, the positive zeta potential and fine particle size would help in prolonging the corneal contact time. Moreover, the PXRD and DSC analyses indicated the decrease of drug crystallinity in the NPs. The NPs were found to provide a biphasic release pattern; initial burst release was followed by the sustained release which fitted best into Peppas and Weibull release kinetics. The NPs also showed higher transcorneal permeation compared to the commercial drug drops. The resulting nanoparticles are promising in reducing dose frequency and improving patient compliance for ocular delivery.

Acknowledgment

The results described in this paper were part of student thesis. The financial support from Drug Applied Research Center of Tabriz University of Medical Sciences under the grant No. 42 is greatly acknowledged. Mitra Jelvehgari received the research grant from Drug Applied Research Center, Tabriz University of Medical Sciences, Tabriz, Iran.

Conflicts of Interest

The authors declare no conflicts of interest.

References

1. Patravale V, Kulkarni R. Nanosuspensions: a promising drug delivery strategy. J Pharm Pharmacol 2004; 56:827-840.
2. Modh N, Mehta D, Parejiya P, Popat A, Barot B. An overview of recent patents on nanosuspension. Recent Pat Drug Deliv Formul 2014; 8:144-154.
3. Pignatello R, Bucolo C, Ferrara P, Maltese A, Puleo A, Puglisi G. Eudragit RS100® nanosuspensions for the ophthalmic controlled delivery of ibuprofen. Eur J Pharm Sci 2002; 16:53-61.
4. Shegokar R, Müller RH. Nanocrystals: industrially feasible multifunctional formulation technology for poorly soluble actives. Int J Pharm 2010; 399:129-139.
5. Leung D, Nelson TD, Rhodes TA, Kwong E. Nano-suspension process. Google Patents; 2012.US 20140256818 A1.
6. Keck CM, Müller RH. Drug nanocrystals of poorly soluble drugs produced by high pressure homogenisation. Euro J Pharm Biopharm 2006; 62:3-16.
7. Tadros T, Izquierdo P, Esquena J, Solans C. Formation and stability of nano-emulsions. Adv Colloid Interface Sci 2004; 108:303-318.
8. Pignatello R, Ricupero N, Bucolo C, Maugeri F, Maltese A, Puglisi G. Preparation and characterization of eudragit retard nanosuspensions for the ocular delivery of cloricromene. AAPS PharmSciTech 2006; 7:E192-E198.
9. Nagarwal RC, Kant S, Singh P, Maiti P, Pandit JK. Polymeric nanoparticulate system: a potential approach for ocular drug delivery. J Control Release 2009; 136:2-13.
10. Pignatello R, Bucolo C, Spedalieri G, Maltese A, Puglisi G. Flurbiprofen-loaded acrylate polymer nanosuspensions for ophthalmic application. Biomaterials 2002; 23:3247-3255.
11. Cholkar K, Patel SP, Vadlapudi AD, Mitra AK. Novel strategies for anterior segment ocular drug delivery. J Ocul Pharmacol Ther 2013; 29:106-123.
12. Bielory L, Friedlaender MH. Allergic conjunctivitis. Immunol Allergy Clin North Am 2008; 28:43-58.
13. Tauber J, Raizman MB, Ostrov CS, Laibovitz RA, Abelson MB, Betts JG, *et al.* A multicenter comparison of the ocular efficacy and safety of diclofenac 0.1% solution with that of ketorolac 0.5% solution in patients with acute seasonal allergic conjunctivitis. J Ocul Pharmacol Ther 1998; 14:137-145.
14. Rathore K, Nema R, Sisodia S. An overview and advancement in ocular drug delivery systems. Int J Pharm Sci Res 2010; 1:11-23.
15. Schafer AI. Effects of nonsteroidal antiinflammatory drugs on platelet function and systemic hemostasis. J Clin Pharmacol 1995; 35:209-219.
16. Gou M, Wu L, Yin Q, Guo Q, Guo G, Liu J, *et al.* Transdermal anaesthesia with lidocaine nano-formulation pretreated with low-frequency ultrasound in rats model. J Nanosci Nanotechnol 2009; 9:6360-6365.
17. Vega E, Egea M, Valls O, Espina M, Garcia M. Flurbiprofen loaded biodegradable nanoparticles for ophtalmic administration. J Pharm Sci 2006; 95:2393-2405.
18. Gilhotra RM, Gilhotra N, Mishra D. Piroxicam bioadhesive ocular inserts: physicochemical characterization and evaluation in prostaglandin-induced inflammation. Curr Eye Res 2009; 34:1065-1073.
19. Varani J, Dame MK, Rittie L, Fligiel SE, Kang S, Fisher GJ, *et al.* Decreased collagen production in chronologically aged skin: roles of age-dependent alteration in fibroblast function and defective mechanical stimulation. Am J Pathol 2006; 168:1861-1868.
20. Sinha V, Bansal K, Kaushik R, Kumria R, Trehan A. Poly-ϵ-caprolactone microspheres and nanospheres: an overview. Int J Pharm 2004; 278:1-23.
21. Bala I, Hariharan S, Kumar MR. PLGA nanoparticles in drug delivery: the state of the art. Crit Rev Ther Drug Carrier Syst 2004; 21:387-422.
22. Abdelwahed W, Degobert G, Fessi H. Investigation of nanocapsules stabilization by amorphous excipients

during freeze-drying and storage. Euro J Pharm Biopharm 2006; 63:87-94.
23. Mainardes RM, Urban MC, Cinto PO, Khalil NM, Chaud MV, Evangelista RC, *et al*. Colloidal carriers for ophthalmic drug delivery. Curr Drug Targets 2005; 6:363-371.
24. Das S, Suresh PK, Desmukh R. Design of Eudragit RL 100 nanoparticles by nanoprecipitation method for ocular drug delivery. Nanomedicine 2010; 6:318-323.
25. Cegnar M, Premzl A, Zavašnik-Bergant V, Kristl J, Kos J. Poly (lactide-co-glycolide) nanoparticles as a carrier system for delivering cysteine protease inhibitor cystatin into tumor cells. Exp Cell Res 2004; 301:223-231.
26. Verwey EJW, Overbeek JTG, Overbeek JTG. Theory of the stability of lyophobic colloids: Courier Corporation; 1999;205 sidor.
27. Pignatello R, Bucolo C, Spedalieri G, Maltese A, Puglisi G. Flurbiprofen-loaded acrylate polymer nanosuspensions for ophthalmic application. Biomaterials 2002; 23:3247-3255.
28. Mandal B. Preparation and physicochemical characterization of Eudragit® RL100 Nanosuspension with potential for Ocular Delivery of Sulfacetamide. University of Toledo May, 2012.
29. Pignatello R, Ricupero N, Bucolo C, Maugeri F. Preparation and characterization of eudragit retard nanosuspensions for the ocular delivery of cloricromene. AAPS PharmSciTech 2006; 7:E192-E198.
30. Malhotra M, Majumdar D. Permeation through cornea. Indian J Exp biol 2001; 39:11-24.
31. Pahuja P, Arora S, Pawar P. Ocular drug delivery system: a reference to natural polymers. Exp Opin Drug Deliv 2012; 9:837-861.
32. Basu S, Adhiyaman R. Preparation and characterization of nitrendipine-loaded Eudragit RL 100 microspheres prepared by an emulsion-solvent evaporation method. Trop J Pharm Res 2008; 7:1033-1041.
33. Ignatious F, Sun L. Electrospun amorphous pharmaceutical compositions. Google Patents 2003. US 20060013869 A1.
34. Swarnakar NK, Jain AK, Singh RP, Godugu C, Das M, Jain S. Oral bioavailability, therapeutic efficacy and reactive oxygen species scavenging properties of coenzyme Q10-loaded polymeric nanoparticles. Biomaterials 2011; 32:6860-6874.
35. Zakeri-Milani P, Loveymi BD, Jelvehgari M, Valizadeh H. The characteristics and improved intestinal permeability of vancomycin PLGA-nanoparticles as colloidal drug delivery system. Colloids Surf B Biointerfaces 2013; 103:174-181.
36. Graeser KA, Strachan CJ, Patterson JE, Gordon KC, Rades T. Physicochemical properties and stability of two differently prepared amorphous forms of simvastatin. Crys Growth Design 2008; 8:128-135.
37. Yadav SK, Mishra S, Mishra B. Eudragit-based nanosuspension of poorly water-soluble drug: formulation and *in vitro–in vivo* evaluation. AAPS PharmSciTech 2012; 13:1031-1044.
38. Costa P, Lobo JS. Influence of dissolution medium agitation on release profiles of sustained-release tablets. Drug Dev Ind Pharm 2001;27:811-817.
39. Aksungur P, Demirbilek M, Denkbaş EB, Vandervoort J, Ludwig A, Ünlü N. Development and characterization of Cyclosporine A loaded nanoparticles for ocular drug delivery: Cellular toxicity, uptake, and kinetic studies. J Control Release 2011; 151:286-294.